

# Chapter 10

## Increasing the Therapeutic Efficacy of Radiotherapy Using Nanoparticles

Ajlan Al Zaki, David Cormode, Andrew Tsourkas, and Jay F. Dorsey

**Abstract** Nanoparticles have garnered significant interest in recent decades for both biomedical imaging and therapeutic applications. The ability to finely tune their sizes and morphologies and modify their surface properties to enable cell-specific receptor targeting for tumor localization and prolonged circulation and the potential of low or reduced toxicity make them attractive agents in both cancer imaging and therapy. Recent studies have shown that nanoparticles in combination with radiation therapy can lead to an increase in the number of DNA double-stranded breaks compared with radiation alone and improve cancer survival in mouse models. With recent advances in imaging modalities as well as new radiation therapy technologies, targeted radiation therapy with nanoparticles is actively being pursued as a strategy to increase the effectiveness of radiation-induced cancer cell death while minimizing damage to normal tissues. This chapter will highlight the past and current developments of nanomedicines used to increase the therapeutic ratio of radiotherapy for in vitro models and in vivo models, the mechanisms of radiation enhancement and interaction of ionizing radiation with nanoparticles, and explore the potential for future integration into clinical radiotherapy practice.

**Keywords** Nanoparticles • Radiosensitizer • Radiotherapy • Imaging • Targeted radiation therapy

---

A. Al Zaki  
George Washington University, School of Medicine and Health Sciences,  
Washington, DC 20052, USA  
e-mail: [ajlan@gwu.edu](mailto:ajlan@gwu.edu)

D. Cormode • J.F. Dorsey (✉)  
Department of Radiation Oncology, Perelman School of Medicine, University of  
Pennsylvania, Philadelphia, PA 19104, USA  
e-mail: [JayD@uphs.upenn.edu](mailto:JayD@uphs.upenn.edu)

A. Tsourkas  
Department of Bioengineering, University of Pennsylvania, Philadelphia, PA 19104, USA  
e-mail: [atsourk@seas.upenn.edu](mailto:atsourk@seas.upenn.edu)

## Overview of Nanoparticles

Nanoparticles are generally defined as objects on the scale of 1–200 nm in diameter. Due to several inherent advantages, they are being investigated extensively for their potential use in the prevention, diagnosis, and treatment of disease. This technology may have the potential to impact medicine, improve quality of life, lower healthcare costs, and ultimately improve patient outcomes [1]. Additional formulations are being introduced into the clinic for many applications including drug delivery [2], immunization [3, 4], image-guided surgery [5, 6], and imaging [7, 8]. With the growing number of nanoparticle formulations and the variety of materials used, the number of distinct nanoplatforms is too numerous to count. Some of the more commonly used nanoparticles include gold nanoparticles (AuNPs) due to their relative ease of synthesis and tunability as well as unique physicochemical properties, superparamagnetic iron oxide nanoparticles (SPIONs) which possess electromagnetic properties that can be utilized for contrast imaging and magnetic therapy, and polymer-based nanoplatforms. Polymer nanoparticles include liposomal formulations, biodegradable polyethylene glycol block polycaprolactone/poly(lactic acid) (PEG-PCL/PLA) micellar nanocarriers, and polymersomes that can be developed to house therapeutic/imaging agents depending on their hydrophilic and hydrophobic properties [9, 10].

Nanoparticles can be synthesized using different materials ranging from inorganic heavy metals with solid cores to amphiphilic polymers with soft shell components. Their shapes and sizes can be finely tuned, and their surfaces can be modified with ligands to help impart stealthiness and deter opsonization by antibodies and complement proteins, thereby increasing circulation times. They can be designed to carry high therapeutic payloads to increase drug accumulation at disease sites while minimizing off-target toxicities, possess unique properties that respond to extracellular microenvironments to improve cellular uptake and drug release, respond to external stimuli such as electromagnetic radiation to help increase site-specific cellular damage or improve image contrast, and easily integrate both therapeutic and diagnostic functionalities enabling both disease detection and treatment within a single administration. The surface coating of the nanoparticles can also influence the interaction of nanoformulations with their extracellular environment as well as specific cell types.

Strategies of nanoparticle targeting can either be classified as passive targeting or active targeting. Passive targeting of nanoparticle formulations is the preferential, but nonspecific, accumulation at a disease site, mediated by the pharmacokinetics of the nanoparticle and the characteristics of the diseased tissue (i.e., without the use of a targeting ligand). The most well-known example of passive targeting is the enhanced permeability and retention effect, which occurs in tumors. As a tumor grows, it will eventually reach a size where metabolic requirements exceed the capability of the existing nearby vascular supply [11]. Consequently, the tumor will respond by secreting factors to promote the process of angiogenesis resulting in the

formation of new blood vessels that facilitate continued growth. Many of these rapidly forming blood vessels are poorly formed, possessing large gaps between endothelial cells, and have non-intact basement membranes, resulting in an increased permeability to structures in the nano-size range [12]. In addition, these actively growing tumors typically have impaired and disorganized lymphatic vessels, causing poor lymphatic drainage which results in the retention of material in the tumor interstitium [11]. This phenomenon of leaky blood vessels and ineffective lymphatic drainage is known as the enhanced permeability and retention (EPR) effect and is the major factor contributing to nanoparticle accumulation in malignancies for diagnostic and therapeutic applications.

Typically many passes through the circulation are necessary in order for an adequate amount of nanoparticles to extravasate at the tumor site for successful imaging and therapy. Therefore, a key design feature for successful passive delivery is a nanoparticle with prolonged *in vivo* circulation times. However, a major obstacle to passive tumor delivery is clearance by the reticuloendothelial system (RES), also commonly known as the mononuclear phagocyte system, which efficiently clears nanoparticulate material from the systemic circulation [13–15]. As a result, for maximal tumor accumulation, nanoparticle formulations must be designed with minimal removal by the RES. Many parameters of a nanoparticle (e.g., size, shape, surface charge, hydrophilicity, and specific coating material) can influence the nanoparticle's interaction with blood and cellular components, thereby affecting blood pool residence times and hence tumor accumulation [16].

The hydrodynamic diameter of a nanoparticle has a strong influence on circulation time and passive nanoparticle tumor penetration [16]. Nanoparticles smaller than 5 nm in diameter are rapidly filtered via the kidneys and excreted in the urine; therefore, their circulation time is very short and their tumor accumulation is low. The size range where nanoparticle blood clearance is minimized, in order to maximize passive delivery by EPR, is in the size range of 5–200 nm. For nanoparticle sizes exceeding roughly 200 nm, extravasation through capillary fenestrations becomes impaired (depending on the tumor type, some tumors have larger or small endothelial fenestrae). In addition, particles of larger size, i.e., >400 nm, are comparable in diameter to capillaries in the lungs and liver and are therefore cleared quickly by these organs, preventing tumor uptake [17].

Surface charge is another important characteristic that affects nanoparticle circulation time and passive tumor delivery by EPR. Previous studies have shown that particles possessing a neutral or mildly negative surface charge exhibit the most favorable circulation profiles and, therefore, optimal tumor accumulation. Particles with strongly negative surface charges interact unfavorably with the RES decreasing circulation time, whereas particles with a positive charge interact electrostatically with the cell membrane and are primarily localized at the site of injection [18].

Finally, the surface coating of the nanoparticle also influences nanoparticle circulation time. Since many groups have demonstrated that incorporation of polyethylene glycol (PEG) into the surface of nanoparticles helps avoid opsonization and

prolong circulation times [19, 20], nanoparticle PEGylation is a very popular method to impart *in vivo* stealth properties [21].

In contrast to passive targeting, active targeting is a nanoparticle delivery strategy whereby the surface of the nanoparticle is modified with targeting ligands to specific receptors or biomarkers such as the folate or the HER2/NEU receptor within the tumor. These strategies achieve tumor delivery via specific interactions with either cancer cells or their microenvironment. Examples of targeting ligands used for such purposes include antibodies, proteins, peptides, aptamers, sugars, and small molecules. However, successful active targeting is still frequently dependent on initial efficient extravasation of the nanoparticles through the permeable tumor endothelium. Therefore, the nanoparticle's physicochemical properties, which influence blood circulation and passive delivery by the EPR effect, are also applicable for designing actively targeted nanoparticles. A consequence of this is that covering the entire surface of a nanoparticle with targeting ligands does not result in optimal targeting, since the stealth properties of the nanoparticle are compromised. Optimal ratios of ligands to surface area need to be determined for individual formulations, but in general occupying 20–40% of the surface with ligands results in the best targeting [22].

Upon successful penetration of nanoparticles into tumor sites, actively targeted agents possess several key advantages compared to passive targeting strategies. While completely passive targeting is dependent on poor lymphatic drainage in order to achieve nanoparticle retention at the tumor site, active targeting can result in greater tumor retention due to specific binding to receptors. In addition, in some cases, the nanoparticle can undergo receptor-mediated internalization and enhance drug delivery to tumor cells as opposed to other cells within the tumor microenvironment such as macrophages that are capable of phagocytosing nanoparticles, thereby reducing delivery to cancer cells [23]. Thus, actively targeted nanoparticles can accumulate at higher concentrations and deliver their payload within cells compared to passively targeted formulations, which are more easily washed out of the tumor interstitial compartment.

Over the past few decades, the combination of nanoparticles with radiotherapy has been a topic of considerable interest (Fig. 10.1). The chemical composition of nanoparticles can be tailored such that they have different mechanisms of interaction between ionizing radiation and nanoparticles. Consequently, studies have been performed to increase the therapeutic efficacy in conventional radiation therapy by using nanoparticles with high atomic numbers ( $Z$ ) as radiation sensitizers that can increase the emission of secondary electrons via their strong photoelectric and Compton effects [25]. Others have looked into the design of nanoparticle drug carriers in which triggered release of chemotherapeutic agents can be controlled by the application of an external radiation beam [26]. Finally, some reports use ionizing radiation to activate nanoparticles that induce cytotoxicity through alternative mechanisms such as phototherapy [27]. This chapter will highlight the most common application of nanoparticles in radiation therapy and their ability to increase the radiobiological effectiveness (RBE).

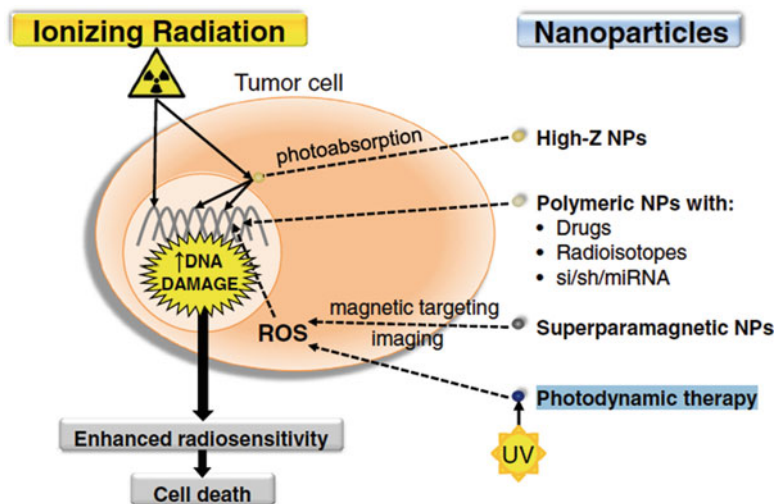


**Fig. 10.1** A schematic depiction of the interaction of nanoparticles with ionizing radiation [24]. With permission from J.W. Bergs et al.

## Safety and Potential Toxicity of Nanoparticles

For the successful clinical translation of nanoparticles, as with any medicine, thorough and careful evaluation of both the safety and pharmacokinetics of the agent is needed. Analysis of nanomaterial toxicity can be done using either *in vitro* or *in vivo* methods. The *in vitro* approach is by far the most commonly used as results can be determined rapidly at a low cost without the use of animals and can provide some insight into the biocompatibility of a nanoplatform. Some commonly accepted methods include the MTT assay for mitochondrial function, the clonogenic assays for cell proliferation and colony studies, and the lactate dehydrogenase assay for evaluating the integrity of the cell membrane, as well as using immunohistochemistry markers for measuring apoptosis and necrosis. While these methods are effective for providing some guidance of potential toxicity profiles, the *in vivo* interaction of nanoparticles with complex and dynamic biological systems cannot be predicted with substantial accuracy. Therefore, *in vivo* testing of nanoparticles is often done to determine the pharmacokinetic and pharmacodynamic profile and to understand their biocompatibility and safety. Methods for *in vivo* evaluation include determining organ biodistribution using multiple time points, blood sample collections for the analysis of circulation half-lives and liver enzymes, changes in appetite or weight, inflammatory cytokines, and histological tissue sectioning for microscopic examination to organ-specific toxicity. Additionally, blood chemistry analytes exist for the evaluation of specific organ toxicity such alanine aminotransferase (ALT), aspartate aminotransferase (AST),

alkaline phosphatase, and total bilirubin for the evaluation of the hepatobiliary system and potential hemolysis.

When designing a nanomedicine for clinical translation, careful consideration of the factors and components that are responsible for the generation of toxicity are in order to maximize the chances of creating a safe agent. For example, silver is generally considered nontoxic when used on a large scale but can be toxic when used on a nanoscale [28]. Furthermore, the pharmacokinetic and pharmacodynamic profiles may provide a basis for potential fates and effects within the human body. For example, particles that are removed by the RES have the potential to cause toxicity and damage in those tissues involved in the clearance of the nanoparticles (liver, spleen, bone marrow). Therefore, the safety of nanoparticles will depend on many parameters including the chemical composition of the nanoformulation, size, shape, reactivity, stability, surface coating, and charge. One must therefore take into account all these properties when evaluating the safety and biocompatibility of nanoparticles.

The general rule of thumb for limiting the potential for nanoparticle toxicity as it relates to nanoparticle size is that they are inversely proportional to one another. This is because nanoparticles become more reactive as they become smaller, and their surface area to volume ratio increases. In addition to size, the nanoparticle shape and surface charge can also contribute to nanoparticle-induced toxicity. Studies have shown that the shape of nanoformulations dictates resulting interactions with biological systems including diffusion, translocation across cell membranes, and biodistribution [29]. For instance, a study evaluating cellular uptake of nanoparticles has shown that spherical AuNPs have a higher uptake in cells compared to gold nanorods [30]. With respect to surface charge, particles with a net negative surface charge tended to be less toxic than those with a positive surface charge, since cell membranes are negatively charged and positively charged particles are taken up by cells more readily. This concept can be exploited to help improve nanoparticle transportation into cancer cells. In one example, nanoparticle surfaces can be linked with a neutral compound that can become positively charged within low-pH microenvironments of certain tumors enabling local intracellular delivery of payload [31]. Surface coating is another important characteristic to consider since it can affect nanoparticle surface charge, hydrophilicity, hydrophobicity, protein adsorption, circulation half-lives, and interaction with specific cell types [32]. The final aspect to take into consideration is nanoparticle stability. This is relevant since nanoparticles can break down in the harsh, acidic environment of lysosomes increasing the concentration of toxic ions within cells, resulting in the buildup of reactive oxygen species [33]. The main mechanisms through which nanoparticles have the potential to exert a toxic effect on biological structures include the generation of free radicals and reactive oxygen species [34], or altering the binding stability and catalytic activity of protein structures, which can ultimately result in the induction of inflammation, genotoxicity, cytotoxicity, and developmental abnormalities [35].

While these nanoparticle characteristics are useful for predicting the potential for toxicity, a clear-cut correlation may not always exist across different nanoparticle platforms and other materials. For example, iron nanoparticles are generally regarded as safe and have been approved by the Food and Drug Administration for the treatment of anemia and contrast-enhanced MRI imaging [36, 37]. On the other hand, it was found

that inclusion of safe iron oxides in emulsions made from edible oils resulted in nanoparticles that could produce toxicity, since the iron oxides catalyzed the oxidation of the oils to produce toxic substances [38]. Similarly, gadolinium used clinically as an MRI contrast agent is well tolerated; however, in patients with compromised kidney function gadolinium, exposure can result in nephrogenic systemic fibrosis [39]. Gold is considered to be very safe. In fact, gold has been used in medical practice throughout history and continues today as a treatment for rheumatoid arthritis [23]. Accordingly, when 12.5 nm AuNPs were administered intraperitoneally into mice every day for 8 days, no evidence of toxicity was observed in any of the studies performed, including survival, behavior, animal weight, organ morphology, blood biochemistry, and tissue histology [40]. In addition studies utilizing 1.9 nm and 0.8 nm AuNPs did not suggest any toxicity in mice [41]. In another study, a toxicological analysis of mice evaluating the intravenous injection of 0.9 nm and 5 nm up to 3 months showed no signs of illness and revealed blood chemistry values within normal limits [42]. Numerous other studies also support the assertion that AuNPs are not toxic to cells [43–48].

## Nanoparticles in Radiation Therapy

Since current irradiation strategies may fail to kill all cancer cells within an irradiated volume, it may be beneficial to selectively enhance radiation at the cellular level. Consequently, many approaches have been developed to enhance the radiation effects specifically within tumors. A radiosensitizer is an agent or drug that increases the cytotoxic susceptibility of cancer cells to radiation therapy. Ideally a radiosensitizer would act specifically on tumor cells while sparing normal tissues, have favorable pharmacokinetic profiles for tumor accumulation prior or during radiation therapy, and be non-toxic. A variety of approaches have been implemented to increase radiation response to help decrease cellular resistance to ionizing radiation while minimizing toxicity to normal tissues. These include oxygen imitators [49–51], thymine analogues [52], inhibitors of cellular repair and cellular processes [53–56], thiol scavengers [52], and nanoparticles [25]. Among these, nanoparticles are favorable because they are able to increase tumor penetration, reduce required radiation doses thereby minimizing adverse effects compared to conventional radiosensitizers, and have been shown to be a promising strategy for increasing the efficiency of radiation therapy [57]. Studies have shown that nanoparticle carriers formed from poly(lactic-co-glycolic acid) PLGA, a biodegradable polymer that can be easily hydrolyzed into the metabolites lactic acid and glycolic acid, containing paclitaxel and etanidazole are able increase radiation sensitivity in tumor cell lines compared to free drug alone or nanoparticles containing only one of the agents [58]. Furthermore, nanoparticles have been used to encapsulate the poorly water-soluble radiosensitizer docetaxel to circumvent the undesirable side effects associated with administration of free drug [59]. Another polymeric nanoparticle that has shown to be a more effective radiation sensitizer *in vivo* compared to free drug alone is Genexol-PM, a polymeric micelle containing paclitaxel used for the treatment of non-small cell lung cancer [60]. However, the most extensively studied nanoparticles for radiation



enhancement are those with high  $Z$  numbers. For example, gold [61], gadolinium [62], bismuth [63], titanium [64], hafnium [65], germanium [66], and platinum [67] have been evaluated for their radiosensitization capabilities. This is because high  $Z$  materials have a higher probability of emitting auger electrons and photoelectrons producing highly oxidizing free radical molecules that cause cellular death. Of all the high  $Z$  material nanoparticles, AuNPs have been the most thoroughly evaluated. The next section will focus primarily on radiation therapy involving nanoformulations containing AuNP.

## Mechanisms of Interaction of Radiation with Nanoparticles

The primary objective of radiation therapy is to deprive cancer cells of their mitotic potential and ultimately promote cancer cell death. The main interaction of X-rays in cells is by Compton scattering, producing secondary high-energy electrons that exert their effects on biological structures. In the cell, DNA is the desired biological target of ionizing radiation. There are two mechanisms by which radiation can interact with DNA. The first is known as direct action where ionizing radiation interacts directly with DNA to cause damage. The second is known as indirect action where ionizing radiation interacts with the surrounding water molecules, generating free radicals, notably hydroxyl radicals [68], which cause lethal damage to cellular DNA. Hydroxyl radicals are generated either directly by the oxidation of water by ionizing radiation or indirectly by the formation of secondary partially reactive oxygen species (ROS). ROS include superoxide ( $O_2^-$ ), hydrogen peroxide ( $H_2O_2$ ), and hydroxyl radicals ( $OH^\cdot$ ). The damage caused can include DNA strand breaks that are initiated by the removal of a deoxyribose hydrogen atom by the activated hydroxyl radical [69]. Excessive damage to cells exposed to radiation can lead to either double-strand breaks (DSB) or single-strand breaks (SSB). DSBs are not the most common type of radiation-induced damage but are regarded as the most serious and potentially lethal. At this stage, some cells will arrest their cell cycle to repair the damage. If the damage is beyond repair then the cell will undergo apoptosis. Alternatively, some cancer cells with mutations in cell cycle checkpoints can continue to proliferate following radiation exposure. However, the majority of these cells will undergo cell death during mitosis as a result of sustained DNA damage and chromosomal defects. The postmitotic or reproductive mode of cell death is considered to be the most prevalent mechanism in cells exposed to ionizing radiation [70–72]. The apoptotic signaling pathway can be initiated in various cellular compartments that include the plasma membrane, cytoplasm, and nucleus [73]. In the plasma membrane, ionizing radiation can promote lipid-oxidative damage through interactions with radiation-induced free radicals resulting in altered ion channels, a buildup in arachidonic acid, and the production of ceramide which is involved in mediating cellular death. Cell death occurs via free radical molecules eliciting cumulative un-repairable lipid-oxidative damage [75].

The mechanism of nanoparticle enhancement, in X-ray therapy, is dependent on the energy of incident ionizing photons and different interactions between the pho-



tons and nanoparticles. The three fundamental mechanisms of radiation enhancement are the photoelectric effect, Compton scattering, and pair production. The photoelectric effect is the predominant mechanism of radiosensitization of high atomic number ( $Z$ ) elements, for photons with energies in the range of 10–500 keV [76]. The cross section of the photoelectric effect varies with the atomic number approximately proportional to  $Z^3$ , meaning that higher  $Z$  atoms will have a larger absorption cross section. The photoelectric effect is also dependent on the energy of the photon, with a maximum cross section when the photon energy is equal to the binding energy of orbital electrons. This effect decreases sharply as energy is increased and varies as  $E^{-3}$ . For example, the binding energies of electrons bound to gold are 79 keV for the inner shells, 13 keV, and 3 keV for outer shells, while those of soft tissue are on the order of 1 keV or lower resulting from the lower atomic number of organic matter. Therefore, gold would absorb significantly more energy than soft tissue in the kilovoltage energy range. When photons with energies in these ranges interact with AuNPs, they can produce electrons, characteristic X-rays of gold atoms, or Auger electrons. Once an atom absorbs a photon, an electron may be emitted resulting in an ionized atom.

When photons of energy greater than the binding energy of an inner shell electron collide, that electron is ejected leaving behind a vacancy in an orbital electron shell. As a result, outer electrons in a higher-energy state fill the vacancy in the lower-energy orbital. This process is accompanied by either a fluorescent photon or an Auger electron ejected from an outer shell with an energy equal to the difference between the two orbital shells. If multiple shells exist within an atom, then further Auger electrons can be generated as outer shell electrons fill in the vacancies. This phenomenon is known as the Auger cascade. The number of Auger electrons emitted is directly proportional to the atomic number. Therefore, high  $Z$  atoms are expected to generate more Auger electrons than elements with lower atomic numbers [77]. The range of these emitted electrons has been calculated to be around tens of nanometers depositing their energy along their path and distributing radiation throughout the system [77]. Furthermore, the Auger electron “shower” can produce highly positively charged ions, causing local Coulomb force fields that can disrupt nearby cellular structures.

The enhancement of radiation with high  $Z$  material was first realized when DNA damage was detected in lymphocytes isolated from patients receiving iodinated contrast agents for X-ray imaging [78]. Since then many other studies have demonstrated that radiation therapy in combination with iodine suppresses tumor growth and improves survival in animal models [79]. Another interesting approach was the incorporation of iodine into cellular DNA yielding a threefold improvement in *in vitro* radiosensitization [80]. However, this strategy is not as effective if insufficient levels of thymine are substituted with iododeoxyuridine. Although the mechanisms of radiation enhancement of gold nanoparticles are not completely understood, it is currently believed that the interaction of X-rays with high  $Z$  atoms induces the release of photoelectrons and Auger electrons [76] (Fig. 10.2).

Given that gold has a higher  $Z$  number (79 vs 53), it is likely that gold as a radiosensitizer would be much more effective than iodine. When photon ener-

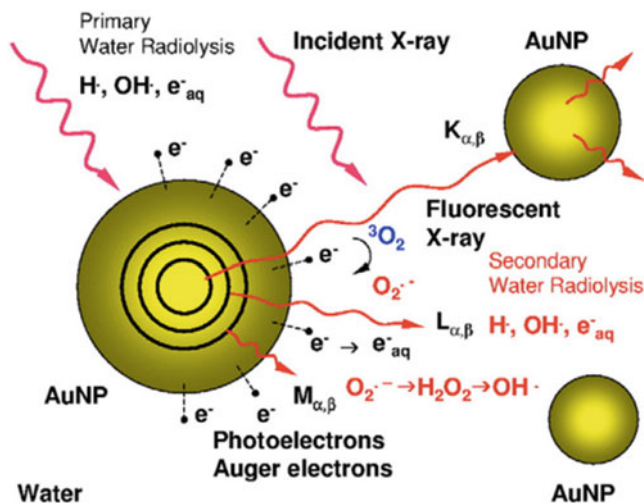


**Fig. 10.2** Schematic depiction of increased generation of reactive oxygen species by the emission of photoelectrons and Auger electrons from AuNPs in the presence of ionizing radiation [74]

gies are greater than 500 keV, Compton effects begin to dominate. The Compton effect is the incoherent or inelastic scattering between an X-ray photon and an electron of an atom. In this interaction, only a part of the energy is transferred to the electron. The resulting emitted electron is known as a Compton electron, leaving behind an ionized atom or molecule. In contrast to photoelectric interactions where most photoelectrons are inner electrons, Compton interactions increase for loosely bound electrons. So most of the Compton electrons are valence electrons. In contrast to Auger electrons, Compton electrons are capable of traveling several hundred microns. For incident photons with energies higher than 1.02 MeV, a process known as pair production dominates where the photon is absorbed by the nucleus with the production of a positron and electron pairs. The probability of pair production increases with the atomic number as  $Z^2$  and linearly with the energy of incident photons. The interaction of charged particles is more complex; however, some studies have speculated that proton-AuNP interactions lead to the increased production of low-energy delta-ray electrons producing a high degree of lethal damage within the cells, thus lowering the surviving fraction of cells [81].

While most nanoparticle radiosensitization has primarily been attributed to their photon absorption capabilities, recent studies highlight that a significant biological component may be responsible for radiosensitization. In the absence of radiation, nanoparticles have been reported to induce ROS that cause oxidative DNA damage [82]. In addition, nanomaterials have been shown to cause alterations in the cell cycle with an increase in cells at the G2/M phase [83]. In a recent study by Kang et al., the nuclear targeting of AuNPs was shown to cause cytokinesis arrest leading

to the failure of complete cell division and apoptosis [84]. Although experimental evidence may suggest the involvement of biological components in radiosensitization, the exact mechanisms are still not clearly understood.

## In Vitro Radiosensitization Using AuNPs

By far the majority of in vitro and in vivo studies analyzing AuNP-mediated radioenhancement rely on passively targeted nanoparticles. One of the earliest studies using gold for radioenhancement was performed by Regulla and colleagues [85]. In this study, enhanced radiation effects were observed in mouse embryo fibroblasts that were exposed to gold surfaces compared to those exposed to polymethyl methacrylate. Secondary electrons were found to travel a range of approximately 10  $\mu\text{m}$ . Following this study, numerous other experimental studies using AuNPs over both orthovoltage (200–500 keV) and megavoltage (>100 keV) ranges have been described. The results of these reports are difficult to compare directly since they were performed using many parameters such as size, shape, surface coating, concentration, radiation type and energy, and origin of cell lines (Table 10.1 adapted from Butterworth et al.). In an attempt to address these issues, Brun and coworkers investigated AuNP radiation enhancement by systematically altering AuNP concentrations, AuNP diameter, and incident X-ray energy (range 14.8–70 keV). They determined that the conditions with the most radiation enhancement were those using larger sized AuNPs, high gold concentration, and 50 keV photons providing dose enhancement factors of 6 [98]. In a separate study, 1.9 nm AuNPs enhanced the response of bovine aortic endothelial cell damage inflicted by X-ray irradiation, with a dose enhancement factor up to 24.6 [91]. While optimal sizes for AuNP radiation therapy may be inconclusive, it is generally accepted that radiation-induced DNA damage will increase with increasing concentrations of AuNPs [99]. In vitro experiments using brachytherapy sources and AuNPs have also been reported and initially demonstrated an increased biological effect with irradiation with values up to 130% greater than without AuNPs [100].

Most photoelectrons, Auger electrons, and other secondary electrons have low energies and a short range in tissues (nm to  $\mu\text{m}$ ) delivering lethal doses in their immediate surroundings [101]. The possibility of having AuNPs target specific cancer cells may increase the production of secondary electrons within the vicinity of DNA molecules, especially if they involve cellular internalization [102]. Chattopadhyay et al. was one of the first to validate this hypothesis by synthesizing trastuzumab-PEG-AuNPs [97]. Briefly, SK-BR-3 cells were irradiated after treatment with either phosphate-buffered saline, PEG-AuNPs, or trastuzumab-PEG-AuNPs. The DNA DSBs as measured by  $\gamma$ -H2AX foci increased 5.1 and 3.3 times for targeted AuNPs compared to cells treated with PBS or PEG-AuNPs, respectively. AuNPs modified with either cysteamine or thioglucose have been shown to have differential accumulation in cancer cells. While cysteamine-modified AuNPs

**Table 10.1** Summary of in vitro radiosensitization experiments using AuNPs

Author	Size (nm)	Concentration	Surface coating	Cell model	Energy source	DEF	SER		
Geng et al. [86]	14	5 nM	Glucose	SK-OV-3	90 kVp	1.002	1.3		
					6 MV	1.00009	1.2		
Jain et al. [87]	1.9	12 $\mu$ M	Thiol	DU-145	160 kVp	1.05	<1.41		
				MDA-231 MB	6 MV	1.0005	<1.29		
				L132	15 MV	1.0005	1.16		
					6 MeV e <sup>-</sup>	1	<1.12		
16 MeV e <sup>-</sup>	1	1.35							
Chithrani et al. [79]	14	1 nM	Citrate	HeLa	220kVp	1.09	1.17–		
	74				6 MV e <sup>-</sup>	1.0008	1.16		
	50				662 keV	1.0006			
Liu et al. [88]	6.1	>1 mM	PEG	CT-26	6 keV e <sup>-</sup>	1	2		
				EMT-6	160 kVp	1.02	1.1		
					6 MV	1.002	1		
Butterworth et al. [89]	1.9	2.4 $\mu$ M	Thiol	DU-145	160kVp	1.01	<1		
		0.24 $\mu$ M		MDA-231 MB					
				AG0-1522					
				Astro					
				L132				1.01	<1.67
				T98G				1.01	<1.97
				MCF-7				1.01	<1.04
				PC-3				1.01	<1
								1.01	<1.91
				1.01				<1.41	
	1.01	<1.07							
	1.01	1.3							
Kong et al. [90]	10.8	15 nM	Glucose	MCF-7	200kVp	1.01	1.3		
			Cysteamine	MCF-10A	662 keV	1.00008	1.6		
					1.2 MV	1.00001			
Rahman et al. [91]	1.9	<1 mM	Thiol	BAEC	80 kV	6.6	20		
					150kV	5.2	1.4		
					6 MV e <sup>-</sup>	1	2.9		
					12 MV e <sup>-</sup>	1	3.7		
Roa et al. [83]	10.8	15 nM	Glucose	DU-145	662 keV	1.00008	>1.5		
Zhang et al. [92]	30	15 nM	Glucose-TGS	DU-145	200kVp	1.0083	>1.3		
						1.0083	>1.5		
Chang et al. [93]	13	11 nM	Citrate	B16F10	6 MV e <sup>-</sup>	1	1		

(continued)

**Table 10.1** (continued)

Author	Size (nm)	Concentration	Surface coating	Cell model	Energy source	DEF	SER
Chien et al. [94]	20	<2 mM	Citrate	CT-26	6 MV e <sup>-</sup>	1	1.19
Zhang et al. [95]	4.8	0.095–3 mM	Citrate	K562	2–10 kR gamma		
	12.1						
	27.3						
	46.6						
Liu et al. [96]	4.7	500 μM	PEG	CT-26	6 MV		1.3–1.6
Chattopadhyay et al. [97]	30	0.3 nM	Trastuzumab-PEG	SK-BR-3	300 kVp		5.1
Brun et al. [98]	8.1	1–5 nM	Citrate	Plasmid DNA	30 kV		<3.3
	20.2				80 kV		
	37.5				80 kV		
	74				100 kV		
	91.7				120 kV		
					150 kV		

*SER* surface enhancement ratio, *DEF* dose enhancement factor

were preferentially limited to the cell membrane of MCF-7 breast cancer cells, glucose-AuNPs are internalized and distributed throughout the cytoplasm [86, 90]. Furthermore, glucose-AuNPs exhibited enhanced irradiation (200 kVp)-induced cell death compared to cysteamine-AuNPs and irradiation alone. Finally, in an independent study, the radiotoxicity of proton therapy with AuNP internalization was increased by approximately 15–20% compared to proton therapy without AuNPs [81]. However, the meaning of these results is not clear, as targeted AuNPs were not compared to nontargeted AuNPs.

## In Vivo Radiosensitization Using AuNPs

In 2004, Hainfeld et al. performed the first animal study evaluating enhanced tumor radiosensitization via AuNPs. Using 1.9 nm AuNPs in combination with 250 kVp X-rays (30 Gy), overall tumor-xenograft mouse survival was 86% versus 20% for radiation alone and 0% for gold only [103]. Since then AuNP radiosensitization has been demonstrated in vivo with murine mammary ductal carcinoma [104], murine squamous cell carcinomas [103], human sarcoma cells [105], and cervical carcinoma (see Table 10.2) [111]. In a study by Zhang and colleagues, in vivo radiosensitization was studied using four different sizes of PEG-AuNPs, and demonstrated that while all sizes can decrease tumor volumes after gamma radiation (5 Gy), the smallest (4.8 nm) and largest (46.6 nm) particles tested had weaker sensitization effects than 12.1 and 27.3 nm [109]. However, in a recent study by Zhang et al.,

**Table 10.2** Summary of in vivo radiosensitization experiments using AuNPs

Author	Size (nm)	AuNP dose (g kg <sup>-1</sup> )	Surface coating	Cell model	Source energy	Dose (Gy)	Predicted DE
Hainfeld et al. [106]	1.9	0–2.7	Thiol	SCCVII	68 kV	30	1.84
					157 kV		1.315
Hebert et al. [104]	5	0–0.675	DTDTPA-Gd	MCF7-L1	150 kV	10	1.01
Chang et al. [93]	13	0–0.036	Citrate	B16F10	MV e <sup>-</sup>	25	1.01
Hainfeld et al. [103]	1.9	0–2.7	Thiol	EMT-6	250 kV	26–30	1.56
Joh et al. [105]	12.4	0–1.25	PEG	HT1080	175 kV	6 Gy	1.16
				U20S			1.07
Joh et al. [107] PLOS	12	0–1.25	PEG	U251	175 kV	20 Gy	1.3
Kim et al. [108]	14	0–0.3	Citrate	CT26	Proton 40 MV	10– 41 Gy	
Zhang et al. [109]	4.8	0–4	PEG	U14	Gamma rays	5 Gy	1.41
							1.65
							1.58
							1.42
							12.1 27.3 46.6
Chattopadhyay et al. [97]	30		Herceptin	MDA-MB-361	100 kV	11 Gy	
Atkinson et al. [110]		n/a	n/a		n/a	6 Gy	
Zhang et al. [111]	1.5	0.01	GSH BSH	U14	662 kV	5 Gy	
Al Zaki et al. [112]	75	0–0.65	PEG	HT1080	175 kV	6 Gy	1.2
McQuade et al. [113]	100	0–0.4	PEG	HT1080	175 kV	6 Gy	1.32
Sun et al. [114]	75	0–0.3	PEG	U251	150 kV	4 Gy	
Vilchis-Juarez et al. [115]	20		RGD, <sup>177</sup> Lu	C6			
Miladi et al. [116]	2		DTDTPA-GD <sub>50</sub>	Osteosarcoma 9LGS	Gamma rays	25 Gy	
					662 kV	20 Gy	

DE dose enhancement

glutathione-coated AuNPs with sizes less than 2 nm have the ability to accumulate preferentially within subcutaneous tumor-bearing mice providing strong radioenhancement for cancer therapy [111]. More recently, Joh et al. showed that PEG-AuNPs and radiation therapy can enhance DNA damage and tumor cell destruction and improve survival in mice with orthotopic glioblastoma multiforme tumors [107]. Intriguingly, they also showed that ionizing radiation could compromise tumor vasculature significantly increasing the accumulation of AuNPs within brain

tumor-bearing mice. All of these strategies mentioned are examples of passive tumor targeting of AuNPs that are reliant on the EPR effect. To our knowledge, a study conducted by Chattopadhyay and coworkers is the only one that has assessed the *in vivo* radioenhancement effects of targeted AuNPs, using a tumor-specific HER-2-targeted nanoplatform [101]. However, the benefits of having targeted AuNPs versus untargeted were not conclusive as there were no *in vivo* comparisons made, and AuNPs were administered via intratumoral injections.

Very few *in vivo* studies have been carried out using MV photon energy beams that are commonly used in radiotherapy. However, some emerging studies are suggestive of the clinical potential of AuNPs in improving outcomes of radiotherapy. Using 6 MV electrons with 13 nm AuNPs, tumor growth was significantly retarded, and survival was prolonged compared to radiation alone in mice with melanoma flank tumors [93]. Increased tumor sensitization with AuNPs has also been demonstrated using proton therapy [108]. Proton beam irradiations of 45 MeV (10–41 Gy) were delivered to subcutaneous colon carcinoma tumors in mice after receiving a single dose of 100–300 mg/kg of AuNPs, which led to a 58–100% 1 year survival versus 11–13% in proton only irradiation.

## Theranostic Agents

There has been a growing trend to integrate both diagnostic and therapeutic agents within a single formulation at the nanoscale level; an approach known as theranostics. The benefit of this combination will enable both disease detection and treatment within a single procedure. Direct visualization of nanoparticle distribution within the tumor can provide guidance for treatment localization, monitor disease progression, and aid in the prediction of therapeutic outcome. Crucial information such as this could invariably be useful for physicians to provide their patients with personalized treatment strategies that help minimize off-target toxicity and improve clinical outcomes. While still at the preclinical stage, a number of studies have demonstrated the use of theranostic nanoformulations for imaging and radiation therapy enhancement. Gadolinium and gold nanoparticles can be used as multimodal agents. Their high *Z* material improves the efficacy of radiation therapy and can be used as contrast agents for magnetic resonance imaging (MRI) and computed tomography (CT), respectively. A multifunctional micellar nanocarrier was prepared by encapsulating both AuNP for radiosensitization and SPIONs for contrast-enhanced imaging (Fig. 10.3). MRI imaging suggested that the heterogeneity of tumor permeability and initial response to radiation therapy was predicted based on the extent of contrast enhancement within the tumor (Fig. 10.4) [113]. Similarly, via the use of gadolinium-based ultra-rigid platforms (USRPs), lung tumors were detected noninvasively using ultrashort echo time magnetic resonance imaging (Fig. 10.5) and improved the mean survival time compared to mice receiving radiation therapy alone (Fig. 10.6) [117]. In another example, a theranostic agent was prepared using magnetic Fe<sub>3</sub>O<sub>4</sub> and silver nanocomposites for simultaneous cancer



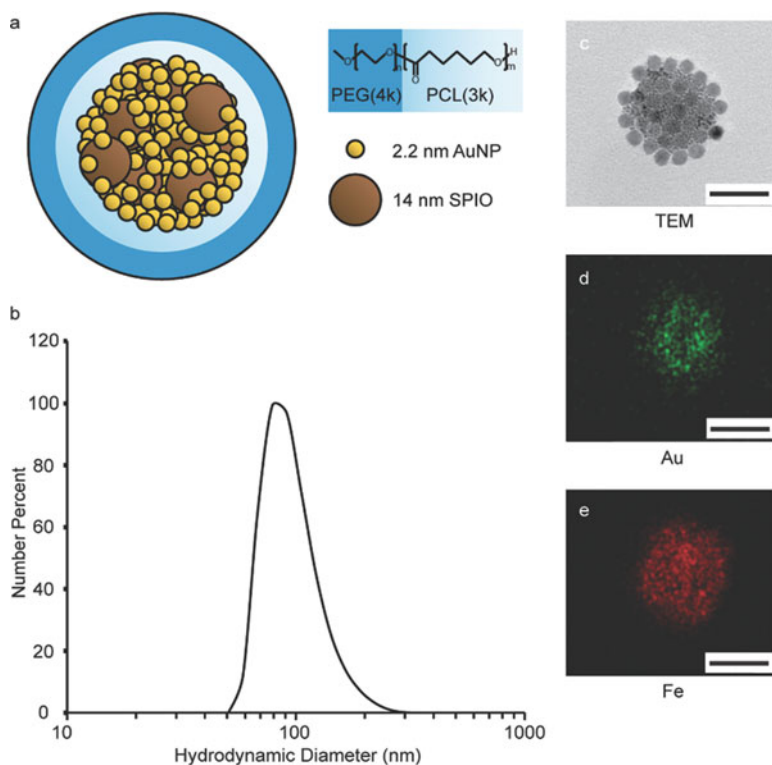


**Fig. 10.3** (a) Schematic depiction of a gold nanoparticle and SPION-loaded polymeric micelles (GSMs). These particles are administered intravenously into tumor-bearing mice. Once particles accumulate within tumors, they provide  $T_2$ -weighted contrast-enhanced MRI imaging for localizing external beam radiation therapy. (b) Dynamic light scattering measurements of GSMs. (c) Electron micrograph of GSMs. (d, e) Energy-dispersive spectroscopy analysis on GSMs with Au and Fe signals detected, respectively

therapy and diagnosis of nasopharyngeal carcinoma [118]. These nanocomposites were conjugated to an epidermal growth factor receptor antibody resulting in an enhancement in radiotoxicity by a factor of 2.26.

While these examples show promise for theranostic agents in cancer therapy, further investigation is warranted. Currently, combining both imaging and therapeutic functionalities significantly increases the cost and complexity of nanoparticle preparation, which adds concerns for commercial viability, altered pharmacokinetics, reduced drug loading capacity, and regulatory hurdles for clinical translation. The incorporation of high sensitivity and quantifiable positron emission tomography (PET) imaging agents onto the surfaces of existing FDA-approved nanoplatforms might be a promising alternative approach to improve nanoparticle biodistribution and antitumor efficacy.

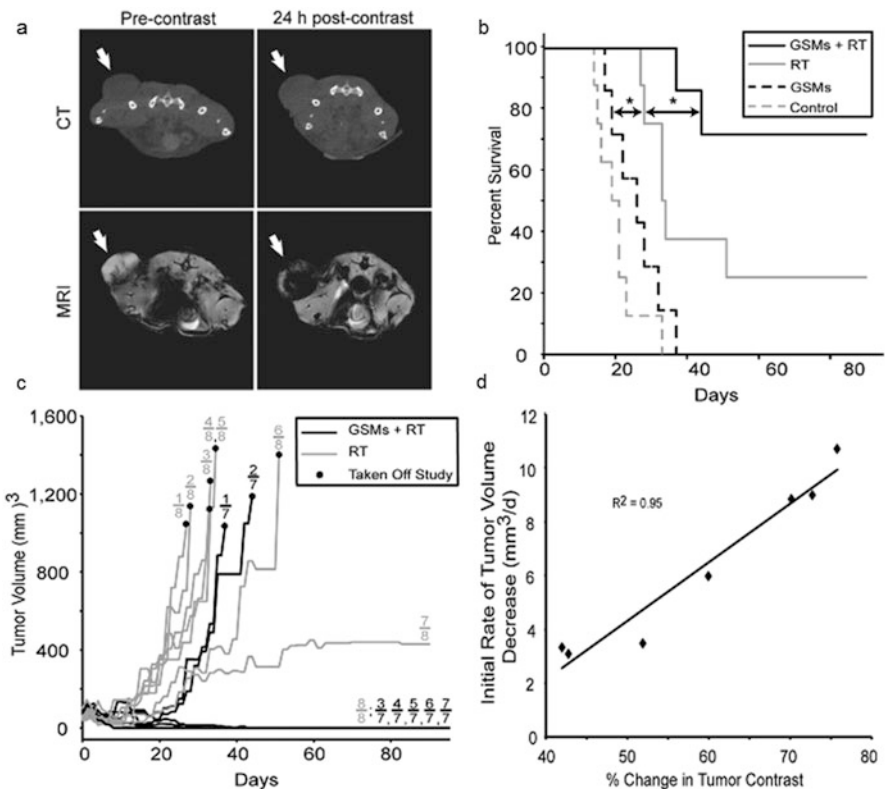


**Fig. 10.4** (a) CT (top) and MR (bottom) imaging of HT1080 flank tumor-bearing mice 24 h postinjection of GSMs. Tumor contrast is enhanced on MR imaging. (b) Kaplan-Meier survival curve in HT1080 tumor-bearing mice receiving no treatment ( $n=8$ ), radiation therapy only ( $n=8$ ), GSMs only ( $n=7$ ), or radiation therapy 24 h post-intravenous injection of GSMs ( $n=7$ ). The radiation dose used was 6 Gy at 150 kVp (c) Plot of average tumor volumes in mice taken over following treatment with GSMs and radiation therapy or radiation therapy alone. (d) Graph of initial rate of tumor volume decrease against the percent change in tumor contrast for mice receiving GSMs plus radiation therapy

### Future/Clinical Translation

With the rapid development and progress of the field of nanotechnology for biomedical applications, there has been wide evaluation of their use for enhanced diagnosis and therapeutic effect in existing treatment modalities. During the past decade, many nanoformulations have been developed as anticancer agents that exert their cytotoxic effects by enhancing the efficacy of radiation therapy. Of the published studies, most have focused on nanoparticles composed of high Z elements like gold, bismuth, and gadolinium. While these approaches have proven successful in preclinical studies, the exact mechanisms of radiosensitization are not yet clearly understood. Therefore, additional studies are needed to

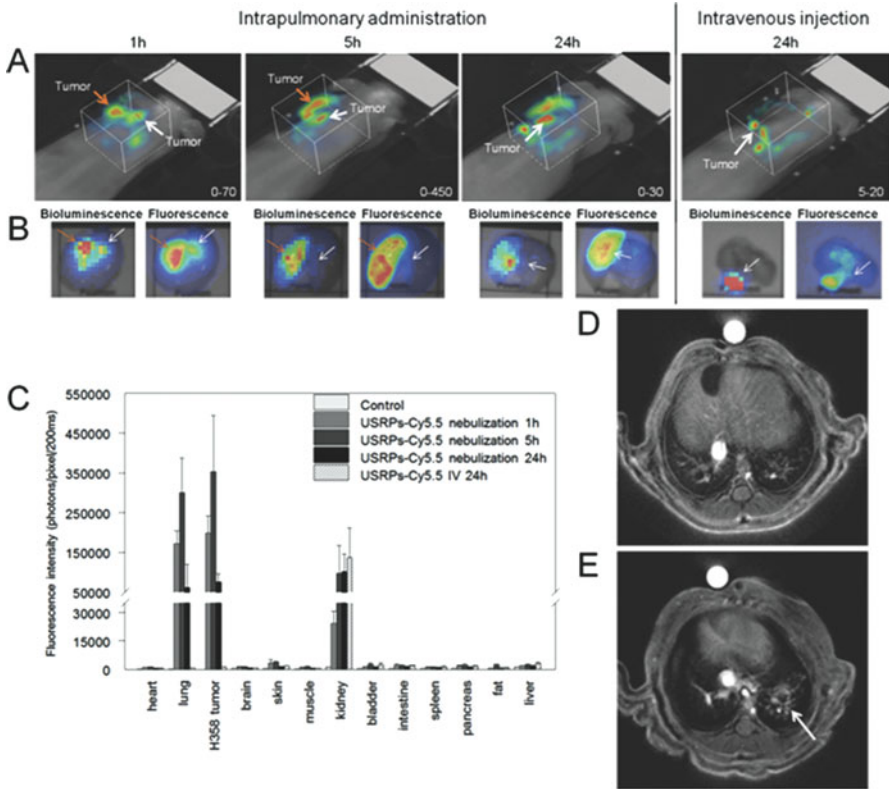


**Fig. 10.5** In vivo imaging of H358-Luc orthotopic lung tumor imaging. (a) Fluorescence imaging of USRPs-CY5.5. (b) Bioluminescence and fluorescence showing the colocalization between H358-Luc tumors and fluorescent USRPs. (c) Organ biodistribution of USRPs following intrapulmonary administration. (d, e) MR imaging of lung tumors pre- and postadministration of USRPs

help elucidate the biological effects exerted by the addition of nanoparticles and therefore direct improved nanoformulation design. Since the majority of studies conducted have focused on irradiation using kilovoltage energies that are limited to superficial tumors and brachytherapy in a clinical setting, the extent of radiosensitization when nanoparticles are exposed to the more clinically utilized megavoltage energies is required. Furthermore, relevant animal models are needed to more accurately mimic clinical disease to determine the potential of nanoparticles for radiosensitization.

Although radiation enhancement has proven to be successful using a variety of nanoparticle formulations, the number of clinical trials using nanoparticles as radiosensitizers is still limited. Current barriers must be overcome that hinder translation of nanoparticles to the clinic. These include the difficulty associated with selection of the optimal nanoplatform, improvement of ligand conjugation efficiencies and technologies, as well as the development of synthetic strategies for nanoparticle

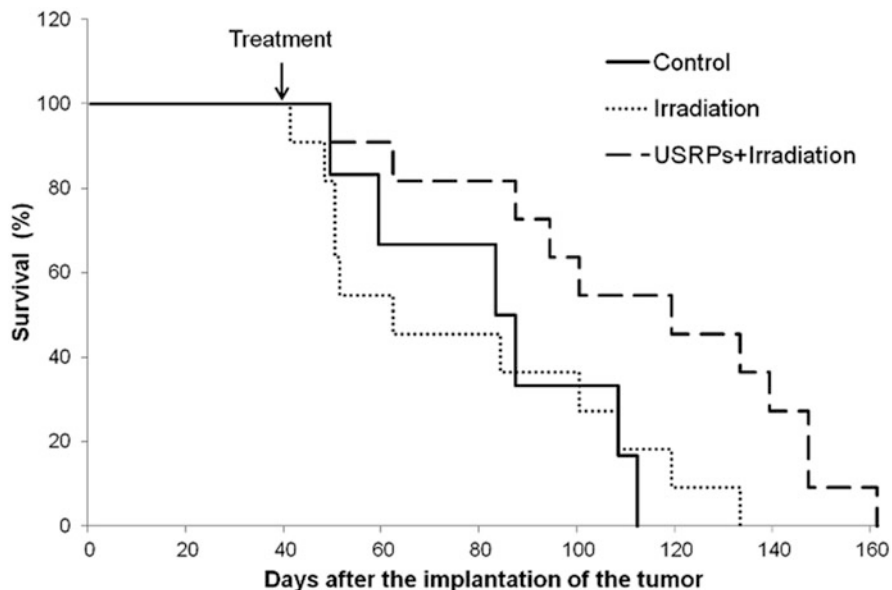


**Fig. 10.6** Survival curve of H358-Luc lung tumor-bearing mice without treatment ( $n=6$ ), treated using a single irradiation only ( $n=11$ ), and irradiated 24 h after intrapulmonary administration of USRPs ( $n=11$ ). Irradiations were performed at 10 Gy

scale-up that follow good manufacturing process with fewer steps, high consistency, and lower costs [119].

Despite these hurdles for clinical translation, some nanotechnology platforms have made it to clinical trials for testing in radiation therapy and are currently being investigated. Phase I clinical trials of hafnium oxide nanoparticles (NBTXR3) were well tolerated and revealed a favorable safety profile with promising signs of antitumor activity. Hafnium oxide nanoparticles (NBTXR3) are currently undergoing phase II/III clinical trials (NCT02379845) after demonstrating efficacy and safety in patients with soft tissue sarcomas in phase I studies [24]. With further advancements in nanoparticle production, purification, and conjugation techniques combined with findings from ongoing and future studies, the number of nanoplatforms that will be translated to clinical studies is expected to increase.

## References

1. Pautler M, Brenner S (2010) Nanomedicine: promises and challenges for the future of public health. *Int J Nanomedicine* 5:803–809
2. Barenholz Y (2012) Doxil(R)—the first FDA-approved nano-drug: lessons learned. *J Control Release* 160:117–134

3. Kanekiyo M et al (2013) Self-assembling influenza nanoparticle vaccines elicit broadly neutralizing H1N1 antibodies. *Nature* 499:102–106
4. des Rieux A, Fievez V, Garinot M, Schneider YJ, Preat V (2006) Nanoparticles as potential oral delivery systems of proteins and vaccines: a mechanistic approach. *J Control Release* 116:1–27
5. Kircher MF et al (2012) A brain tumor molecular imaging strategy using a new triple-modality MRI-photoacoustic-Raman nanoparticle. *Nat Med* 18:829–834
6. Jiang S, Gnanasammandhan MK, Zhang Y (2010) Optical imaging-guided cancer therapy with fluorescent nanoparticles. *J R Soc Interface* 7:3–18
7. Reddy GR et al (2006) Vascular targeted nanoparticles for imaging and treatment of brain tumors. *Clin Cancer Res* 12:6677–6686
8. Cheng Z, Al Zaki A, Hui JZ, Muzykantov VR, Tsourkas A (2012) Multifunctional nanoparticles: cost versus benefit of adding targeting and imaging capabilities. *Science* 338:903–910
9. Torchilin VP (2002) PEG-based micelles as carriers of contrast agents for different imaging modalities. *Adv Drug Deliv Rev* 54:235–252
10. Prabhu RH, Patravale VB, Joshi MD (2015) Polymeric nanoparticles for targeted treatment in oncology: current insights. *Int J Nanomedicine* 10:1001–1018
11. Maeda H, Wu J, Sawa T, Matsumura Y, Hori K (2000) Tumor vascular permeability and the EPR effect in macromolecular therapeutics: a review. *J Control Release* 65:271–284
12. Konerding MA, Fait E, Gaumann A (2001) 3D microvascular architecture of pre-cancerous lesions and invasive carcinomas of the colon. *Br J Cancer* 84:1354–1362
13. Balasubramanian SK, Jittiwat J, Manikandan J, Ong CN, Yu LE, Ong WY (2010) Biodistribution of gold nanoparticles and gene expression changes in the liver and spleen after intravenous administration in rats. *Biomaterials* 31(8):2034–2042
14. Cho WS, Cho M, Jeong J, Choi M, Cho HY, Han BS, Kim SH, Kim HO, Lim YT, Chung BH (2009) Acute toxicity and pharmacokinetics of 13 nm-sized PEG-coated gold nanoparticles. *Toxicol Appl Pharmacol* 236(1):16–24
15. Niidome T, Yamagata M, Okamoto Y, Akiyama Y, Takahashi H, Kawano T, Katayama Y, Niidome Y (2006) PEG-modified gold nanorods with a stealth character for in vivo applications. *J Control Release* 114(3):343–347
16. Frank A, Pridgen E, Molnar LK, Farokhzad OC (2008) Factors affecting the clearance and biodistribution of polymeric nanoparticles. *Mol Pharm* 5(4):505–515
17. Blanco E, Shen H, Ferrari M (2015) Nanoparticle size, shape and surface charge dictate biodistribution among the different organs including the lungs, liver, spleen and kidneys. *Nat Biotechnol* 33:941–951
18. He C, Hu Y, Yin L, Tang C, Yin C (2010) Effects of particle size and surface charge on cellular uptake and biodistribution of polymeric nanoparticles. *Biomaterials* 31(13):3657–3666
19. Lemarchand C, Gref R, Couvreur P (2004) Polysaccharide-decorated nanoparticles. *Eur J Pharm Biopharm* 58:327–341
20. Lemarchand C, Gref R, Passirani C, Garcion E, Petri B, Muller R, Costantini D, Couvreur P (2006) Influence of polysaccharide coating on the interactions of nanoparticles with biological systems. *Biomaterials* 27:108–118
21. Koo OM, Rubinstein I, Onyuksel H (2005) Role of nanotechnology in targeted drug delivery and imaging: a concise review. *Nanomedicine* 1:193–212
22. Elias DR, Poloukhine A, Popik V, Tsourkas A (2013) Effect of ligand density, receptor density, and nanoparticle size on cell targeting. *Nanomedicine* 9(2):194–201
23. Xu S, Olenyuk BZ, Okamoto CT, Hamm-Alvarez SF (2013) Targeting receptor-mediated endocytic pathways with nanoparticles: rationale and advances. *Adv Drug Deliv Rev* 65(1):121–138
24. Bergs JWJ, Wacker MG, Hehlhans S, Piiper A, Multhoff G, Rodel C, Rodel F (2015) The role of recent nanotechnology in enhancing the efficacy of radiation therapy. *Biochim Biophys Acta* 1856(1):130–143
25. Retif P, Pinel S, Toussaint M, Frochot C, Chouikrat R, Bastogne T, Barberi-Heyob M (2015) Nanoparticles for radiation therapy enhancement: the key parameters. *Theranostics* 5(9):1030–1044

26. Starkewolf ZB, Miyachi L, Wong J, Guo T (2013) X-ray triggered release of doxorubicin from nanoparticle drug carriers for cancer therapy. *Chem Commun* 49:2545–2547
27. Chen W, Zhang J (2006) Using nanoparticles to enable simultaneous radiation and photodynamic therapies for cancer treatment. *J Nanosci Nanotechnol* 6(4):1159–1166
28. AshaRani PV, Kah Mun GL, Hande MP, Valiyaveetil S (2009) Cytotoxicity and genotoxicity of silver nanoparticles in human cells. *ACS Nano* 3(2):279–290
29. Chithrani BD, Ghazani AA, Chan WCW (2006) Determining the size and shape dependence of gold nanoparticle uptake into mammalian cells. *Nano Lett* 6(4):662–668
30. Arnida, Janat-Amsbury MM, Ray A, Peterson CM, Ghandehari H (2011) Geometry and surface characteristics of gold nanoparticles influence their biodistribution and uptake by macrophages. *Eur J Pharm Biopharm* 77(3):417–423
31. Cheng Z, Al Zaki A, Hui JZ, Muzykantov VR, Tsourkas A (2012) Multifunctional nanoparticles: cost versus benefit of adding targeting and imaging capabilities. *Science* 338(6109):903–910
32. Albanese A, Tang PS, Chan WCW (2012) The effect of nanoparticle size, shape, and surface chemistry on biological systems. *Annu Rev Biomed Eng* 14:1–16
33. Petros RA, DeSimone JD (2010) Strategies in the design of nanoparticles for therapeutic applications. *Nature* 9:615–627
34. Fu PP, Xia Q, Hwang HM, Ray PC, Yu H (2014) Mechanisms of nanotoxicity: generation of reactive oxygen species. *J Food Drug Anal* 22(1):64–75
35. Park MV, Neigh AM, Vermeulen JP, de la Fonteyne LJ, Verharen HW, Briede JJ, van Loveren H, de Jong WH (2011) The effect of particle size on the cytotoxicity, inflammation, developmental toxicity and genotoxicity of silver nanoparticles. *Biomaterials* 32(36):9810–9817
36. Schwenk MH (2010) Ferumoxytol: A new intravenous iron preparation for the treatment of iron deficiency anemia in patients with chronic kidney disease. *Pharmacotherapy* 30(1):70–79
37. Thomas R, Park IK, Jeong YY (2013) Magnetic iron oxide nanoparticles for multimodal imaging and therapy of cancer. *Int J Mol Sci* 14(8):15910–15930
38. van Tilborg GAF, Cormode DP, Jarzyna PA, van der Toorn A, van der Pol SMA, van Bloois L, Fayad ZA, Storm G, Mulder WJM, de Vries HE, Dijkhuizen RM (2012) Nanoclusters of iron oxide: effect of core composition on structure, biocompatibility and cell labeling efficacy. *Bioconj Chem* 23:941–950
39. Tommaro A, Narcisi A, Tuchinda P, Sina B (2015) Nephrogenic systemic fibrosis following gadolinium administration. *Cuitis* 96(1):E23–E25
40. Lasagna-Reeves C, Gonzalez-Romero D, Barria MA, Olmedo I, Clos A, Sadagopa Ramanujam VM, Urayama A, Vergara L, Kogan MJ, Soto C (2010) Bioaccumulation and toxicity of gold nanoparticles after repeated administration in mice. *Biochem Biophys Res Commun* 393(4):649–655
41. Hainfeld JF, Dilmanian FA, Slatkin DN, Smilowitz HM (2008) Radiotherapy enhancement with gold nanoparticles. *J Pharm Pharmacol* 60(8):977–985
42. Al Zaki A, Hui JZ, Higbee E, Tsourkas A (2015) Biodistribution, clearance, and toxicology of polymeric micelles loaded with 0.9 or 5 nm gold nanoparticles. *J Biomed Nanotechnol* 11(10):1836–1846
43. Chen PC, Mwakwari SC, Oyeler AK (2008) Gold nanoparticles: from nanomedicine to nanosensing. *Nanotechnol Sci Appl* 1:45–66
44. Connor EE, Mwachuka J, Gole A, Murphy CJ, Wyatt MD (2005) Gold nanoparticles are taken up by human cells but do not cause acute cytotoxicity. *Small* 1(3):325–327
45. Lewinski N, Colvin V, Drezek R (2008) Cytotoxicity of nanoparticles. *Small* 4(1):26–49
46. Pan Y, Neuss S, Leifert A, Fischler M, Wen F, Simon U, Schmid G, Brandau W, Jahnen-Dechent W (2007) Size-dependent cytotoxicity of gold nanoparticles. *Small* 3(11):1941–1949
47. Shukla R, Bansal V, Chaudhary M, Basu A, Bhonde RR, Sastry M (2005) Biocompatibility of gold nanoparticles and their endocytotic fate inside the cellular compartment: a microscopic overview. *Langmuir* 21(23):10644–10654
48. Tkachenko AG, Xie H, Coleman D, Glomm W, Ryan J, Anderson MF, Franzen S, Feldheim DL (2003) Multifunctional gold nanoparticle-peptide complexes for nuclear targeting. *J Am Chem Soc* 125(16):4700–4701

49. Chassagne D, Charreau I, Sancho-Garnier H, Eschwege F, Malaise EP (1992) First analysis of tumor regression for the European randomized trial of etanidazole combined with radiotherapy in head and neck carcinomas. *Int J Radiat Oncol Biol Phys* 22:581–584
50. Murayama C et al (1993) Radiosensitization by a new potent nucleoside analog: 1-(1',3',4'-trihydroxy-2'-butoxy)methyl-2-nitroimidazole(RP-343). *Int J Radiat Oncol Biol Phys* 26:433–443
51. Murayama C et al (1989) Radiosensitization by a new nucleoside analogue: 1-[2-hydroxy-1-(hydroxymethyl)ethoxy]methyl-2-nitroimidazole (RP-170). *Int J Radiat Oncol Biol Phys* 17:575–581
52. Wardman P (2007) Chemical radiosensitizers for use in radiotherapy. *Clin Oncol (R Coll Radiol)* 19:397–417
53. Kvols LK (2005) Radiation sensitizers: a selective review of molecules targeting DNA and non-DNA targets. *J Nucl Med* 46(Suppl 1):187S–190S
54. Servidei T et al (2001) The novel trinuclear platinum complex BBR3464 induces a cellular response different from cisplatin. *Eur J Cancer* 37:930–938
55. Richmond RC (1984) Toxic variability and radiation sensitization by dichlorodiammineplatinum(II) complexes in *Salmonella typhimurium* cells. *Radiat Res* 99:596–608
56. Amorino GP, Freeman ML, Carbone DP, Lebwohl DE, Choy H (1999) Radiopotentiality by the oral platinum agent, JM216: role of repair inhibition. *Int J Radiat Oncol Biol Phys* 44:399–405
57. Dorsey JF, Sun L, Joh DY, Witztum A, Al Zaki A, Kao GD, Alonso-Basanta M, Avery S, Tsourkas A, Hahn SM (2013) Gold nanoparticles in radiation research: potential applications for imaging and radiosensitization. *Transl Cancer Res* 2(4):280–291
58. Jin C, Bai L, Wu H, Tian F, Guo G (2007) Radiosensitization of paclitaxel, etanidazole and paclitaxel+etanidazole nanoparticles on hypoxic human tumor cells in vitro. *Biomaterials* 28(25):3723–3730
59. Werner ME, Copp JA, Karve S et al (2011) Folate-targeted polymeric nanoparticle formulation of docetaxel is an effective molecularly targeted radiosensitizer with efficacy dependent on the timing of radiotherapy. *ACS Nano* 5:8990–8998
60. Werner ME, Cummings ND, Sethi M et al (2013) Preclinical evaluation of Genexol-PM, a nanoparticle formulation of paclitaxel, as a novel radiosensitizer for the treatment of non-small cell lung cancer. *Int J Radiat Oncol Biol Phys* 86:463–468
61. Jeremic B, Aguerri AR, Filipovic N (2013) Radiosensitization by gold nanoparticles. *Clin Transl Oncol* 15:593–601
62. Young SW, Qing F, Harriman A et al (1996) Gadolinium(III) texaphyrin: a tumor selective radiation sensitizer that is detectable by MRI. *Proc Natl Acad Sci U S A* 93:6610–6615
63. Yao MH, Ma M, Chen Y, Jia XQ, Xu G, Xu HX, Chen HR, Wu R (2014) Multifunctional BiS23/PLGA nanocapsule for combined HIFU/radiation therapy. *Biomaterials* 35(28):8197–8205
64. Mirjolet C, Papa AL, Crehange G, Raguin O, Seignez C, Paul C, Truc G, Maingon P, Millot N (2013) The radiosensitization effect of titanate nanotubes as a new tool in radiation therapy for glioblastoma: a proof-of-concept. *Radiother Oncol* 108(1):136–142
65. Maggiorella L, Barouch G, Devaux C, Pottier A, Deutsch E, Bourhis J, Borghi E, Levy L (2012) Nanoscale radiotherapy with hafnium oxide nanoparticles. *Future Oncol* 8(9):1167–1181
66. Lin MH, Hsu TS, Yang PM, Tsai MY, Perng TP, Lin LY (2009) Comparison of organic and inorganic germanium compounds in cellular radiosensitivity and preparation of germanium nanoparticles as a radiosensitizer. *Int J Radiat Biol* 85:214–226
67. Porcel E, Liehn S, Remita H, Usami N, Kobayashi K, Furusawa Y et al (2010) Platinum nanoparticles: a promising material for future cancer therapy? *Nanotechnology* 21:85103
68. Riley PA (1994) Free radicals in biology: oxidative stress and the effects of ionizing radiation. *Int J Radiat Biol* 65:27–33
69. Balasubramanian B, Pogozelski WK, Tullius TD (1998) DNA strand breaking by the hydroxyl radical is governed by the accessible surface areas of the hydrogen atoms of the DNA backbone. *Proc Natl Acad Sci U S A* 95:9738–9743



70. Steel GG, McMillan TJ, Peacock JH (1989) The 5Rs of radiobiology. *Int J Radiat Biol* 56:1045–1048
71. Radford IR, Broadhurst S (1986) Enhanced induction by X-irradiation of DNA double-strand breakage in mitotic as compared with S-phase V79 cells. *Int J Radiat Biol Relat Stud Phys Chem Med* 49:909–914
72. Bedford JS (1991) Sublethal damage, potentially lethal damage, and chromosomal aberrations in mammalian cells exposed to ionizing radiations. *Int J Radiat Oncol Biol Phys* 21:1457–1469
73. Bedresen DE (2000) Apoptosis: overview and signal transduction pathways. *J Neurotrauma* 17:801–810
74. Misawa M, Takahashi J (2011) Generation of reactive oxygen species induced by gold nanoparticles under X-ray and UV irradiations. *Nanomedicine* 7:604–614
75. Giusti AM, Raimondi M, Ravagnan G, Sapora O, Parasassi T (1998) Human cell membrane oxidative damage induced by single and fractionated doses of ionizing radiation: a fluorescence spectroscopy study. *Int J Radiat Biol* 74:595–605
76. Meshahi A (2010) A review on gold nanoparticles radiosensitization effect in radiation therapy of cancer. *Rep Prac Oncol Radiother* 15:176–180
77. Kobayashi K, Usami N, Porcel E, Lacombe S, Le Sech C (2010) Enhancement of radiation effect by heavy elements. *Mutat Res* 704:123–131
78. Adams FH, Norman A, Mello RS, Bass D (1977) Effect of radiation and contrast media on chromosomes. Preliminary report. *Radiology* 124:823–826
79. Chithrani DB et al (2010) Gold nanoparticles as radiation sensitizers in cancer therapy. *Radiat Res* 173:719–728
80. Nath R, Bongiorno P, Rockwell S (1990) Iododeoxyuridine radiosensitization by low- and high-energy photons for brachytherapy dose rates. *Radiat Res* 124:249–258
81. Polf JC et al (2011) Enhanced relative biological effectiveness of proton radiotherapy in tumor cells with internalized gold nanoparticles. *Appl Phys Lett* 98:193702
82. Butterworth KT, McMahon SJ, Currell FJ, Prise KM (2012) Physical basis and biological mechanisms of gold nanoparticle radiosensitization. *Nanoscale* 4:4830–4838
83. Roa W et al (2009) Gold nanoparticle sensitize radiotherapy of prostate cancer cells by regulation of the cell cycle. *Nanotechnology* 20:375101
84. Kang B, Mackey MA, El-Sayed MA (2010) Nuclear targeting of gold nanoparticles in cancer cells induces DNA damage, causing cytokinesis arrest and apoptosis. *J Am Chem Soc* 132:1517–1519
85. Regulla DF, Hieber LB, Seidenbusch M (1998) Physical and biological interface dose effects in tissue due to X-ray-induced release of secondary radiation from metallic gold surfaces. *Radiat Res* 150:92–100
86. Geng F et al (2011) Thio-glucose bound gold nanoparticles enhance radio-cytotoxic targeting of ovarian cancer. *Nanotechnology* 22:285101
87. Jain S et al (2011) Cell-specific radiosensitization by gold nanoparticles at megavoltage radiation energies. *Int J Radiat Oncol Biol Phys* 79:531–539
88. Liu CJ et al (2010) Enhancement of cell radiation sensitivity by pegylated gold nanoparticles. *Phys Med Biol* 55:931–945
89. Butterworth KT et al (2010) Evaluation of cytotoxicity and radiation enhancement using 1.9 nm gold particles: potential application for cancer therapy. *Nanotechnology* 21:295101
90. Kong T et al (2008) Enhancement of radiation cytotoxicity in breast-cancer cells by localized attachment of gold nanoparticles. *Small* 4:1537–1543
91. Rahman WN et al (2009) Enhancement of radiation effects by gold nanoparticles for superficial radiation therapy. *Nanomedicine* 5:136–142
92. Zhang X et al (2008) Enhanced radiation sensitivity in prostate cancer by gold-nanoparticles. *Clin Invest Med* 31:E160–E167
93. Chang MY et al (2008) Increased apoptotic potential and dose-enhancing effect of gold nanoparticles in combination with single-dose clinical electron beams on tumor-bearing mice. *Cancer Sci* 99:1479–1484

94. Chien, C.C. et al. (2006) Synchrotron radiation instrumentation. Ninth international conference on synchrotron radiation instrumentation. vol 879
95. Zhang XD et al (2009) Irradiation stability and cytotoxicity of gold nanoparticles for radiotherapy. *Int J Nanomedicine* 4:165–173
96. Liu CJ et al (2008) Enhanced x-ray irradiation-induced cancer cell damage by gold nanoparticles treated by a new synthesis method of polyethylene glycol modification. *Nanotechnology* 19:295104
97. Chattopadhyay N et al (2010) Design and characterization of HER-2-targeted gold nanoparticles for enhanced X-radiation treatment of locally advanced breast cancer. *Mol Pharm* 7:2194–2206
98. Brun E, Sanche L, Sicard-Roselli C (2009) Parameters governing gold nanoparticle X-ray radiosensitization of DNA in solution. *Colloids Surf B Biointerfaces* 72:128–134
99. Zheng Y, Hunting DJ, Ayotte P, Sanche L (2008) Radiosensitization of DNA by gold nanoparticles irradiated with high-energy electrons. *Radiat Res* 169:19–27
100. Ngwa W et al (2013) In vitro radiosensitization by gold nanoparticles during continuous low-dose-rate gamma irradiation with I-125 brachytherapy seeds. *Nanomedicine* 9:25–27
101. Chattopadhyay N et al (2013) Molecularly targeted gold nanoparticles enhance the radiation response of breast cancer cells and tumor xenografts to X-radiation. *Breast Cancer Res Treat* 137:81–91
102. Hossain M, Su M (2012) Nanoparticle location and material dependent dose enhancement in X-ray radiation therapy. *J Phys Chem C Nanomater Interfaces* 116:23047–23052
103. Hainfeld JF, Slatkin DN, Smilowitz HM (2004) The use of gold nanoparticles to enhance radiotherapy in mice. *Phys Med Biol* 49:N309–N315
104. Hebert EM, Deboutiere PJ, Lepage M, Sanche L, Hunting DJ (2010) Preferential tumour accumulation of gold nanoparticles, visualised by Magnetic Resonance Imaging: radiosensitisation studies in vivo and in vitro. *Int J Radiat Biol* 86:692–700
105. Joh DY et al (2013) Theranostic gold nanoparticles modified for durable systemic circulation effectively and safely enhance the radiation therapy of human sarcoma cells and tumors. *Transl Oncol* 6:722–731
106. Hainfeld JF et al (2010) Gold nanoparticles enhance the radiation therapy of a murine squamous cell carcinoma. *Phys Med Biol* 55:3045–3059
107. Joh DY et al (2013) Selective targeting of brain tumors with gold nanoparticle-induced radiosensitization. *PLoS One* 8, e62425
108. Kim JK et al (2012) Enhanced proton treatment in mouse tumors through proton irradiated nanoradiator effects on metallic nanoparticles. *Phys Med Biol* 57:8309–8323
109. Zhang XD et al (2012) Size-dependent radiosensitization of PEG-coated gold nanoparticles for cancer radiation therapy. *Biomaterials* 33:6408–6419
110. Atkinson RL et al (2010) Thermal enhancement with optically activated gold nanoshells sensitizes breast cancer stem cells to radiation therapy. *Sci Transl Med* 2:55ra79
111. Zhang XD et al (2014) Enhanced tumor accumulation of sub-2 nm gold nanoclusters for cancer radiation therapy. *Adv Healthc Mater* 3:133–141
112. Al Zaki A, Joh D, Cheng Z, de Barros AL, Kao GD, Dorsey JF, Tsourkas A (2014) Gold-loaded polymeric micelles for computed tomography-guided radiation therapy treatment and radiosensitization. *ACS Nano* 8(1):104–112
113. McQuade C, Al Zaki A, Desai Y, Vido M, Sakhuja T, Cheng Z, Hickey R, Joh D, Park S-J, Kao GD, Dorsey JF, Tsourkas A (2015) A multi-functional nanoplatform for imaging, radiotherapy, and the prediction of therapeutic response. *Small* 11(7):834–843
114. Sun L, Joh DY, Al Zaki A, Stangl M, Murty S, Davis JJ, Baumann BC, Alonso-Basanta M, Kao GD, Tsourkas A, Dorsey JF (2015) Theranostic application of mixed gold and superparamagnetic iron oxide nanoparticle micelles in glioblastoma multiforme. *J Biomed Nanotechnol* 11:1–10
115. Vilchis-Juarez A, Ferro-Flores G, Santos-Cuevas C, Morales-Avila E, Ocampo-Garcia B, Diaz-Nieto L, Luna-Gutierrez M, Jimenez-Mancilla N, Pedraza-Lopez M, Gomez-Olivan L (2014)

- Molecular targeting radiotherapy with cyclo-RGDfK(C) peptides conjugated to  $^{177}\text{Lu}$ -labeled gold nanoparticles in tumor bearing mice. *J Biomed Nanotechnol* 10:395–404
116. Miladi I, Alric C, Dufort S, Mowat P, Dutour A, Mandon C, Laurent G, Bräuer-Krisch E, Herath N, Coll JL, Dutreix M, Lux F, Bazzi R, Billotey C, Janier M, Perriat P, Le Duc G, Roux S, Tillement O (2014) The in vivo radiosensitizing effect of gold nanoparticles based MRI contrast agents. *Small* 10(6):1116–1124
  117. Dufort S, Bianchi A, Henry M, Lux F, Le Duc G, Josserand V, Louis C, Perriat P, Cremillieux Y, Tillement O, Coll JL (2015) Nebulized gadolinium-based nanoparticles: A theranostic approach for lung tumor imaging and radiosensitization. *Small* 11(2):215–221
  118. Zhao D, Sun X, Tong J, Ma J, Bu X, Xu R, Fan R (2012) A novel multifunctional nanocomposite C225-conjugated  $\text{Fe}_3\text{O}_4/\text{Ag}$  enhances the sensitivity of nasopharyngeal carcinoma cells to radiotherapy. *Acta Biochim Biophys Sin (Shanghai)* 44(8):678–684
  119. Aillon KL, Xie Y, El-Gendy N, Berkland CJ, Forrest ML (2009) Effects of nanomaterial physicochemical properties on in vivo toxicity. *Adv Drug Deliv Rev* 61:457–466